# 2

## Solid Earth Modelling Programme (SEMP)

*Global Positioning System (GPS) based Geodesy had become capable of yielding sub-cm precision in location by the early 1990s and the possibility of it being used to determine crustal strain rates in India was recognised at C-MMACS in 1993 following the Khillari earthquake. Research at C-MMACS has since yielded fairly well constrained figures for the velocity of the Indian plate and partitioning of strain from Kanya-Kumari to Ladakh in the trans-Himalya. Over the years C-MMACS has also taken up the ardous task of setting up GPS stations in remote locations in the country to generate required data base, and to extend application of GPS technology to other areas.*

### *Highlights*

*The year 2004-05 for SEMP has seen a spectrum of activities in the areas of seismic data analysis, study of tectonics in the Himalayan region and applications and analysis of GPS data. C-MMACS had also carried out a quick response analysis of GPS measurements in Andaman Nicobar Islands following the devastating Sumatra earthquake of 26th December, 2004.*

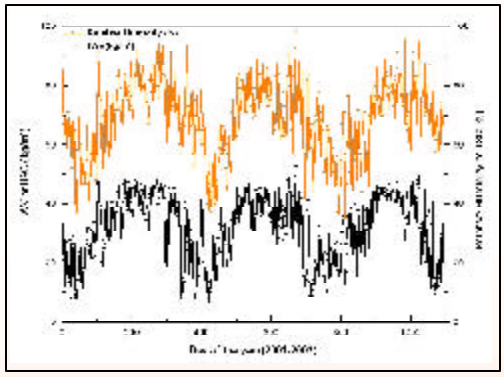

*Time series of GPS derived IWV estimates and ground estimates humidity for Bangalore*

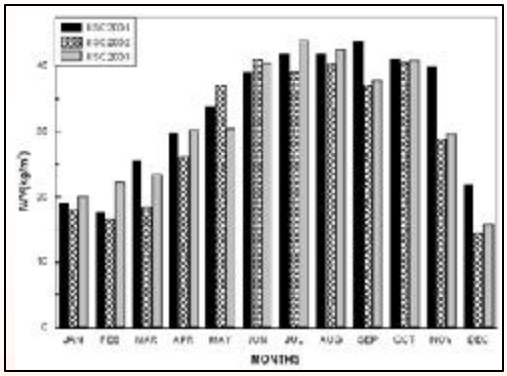

*Inter annual variability of GPS derived IWV for Bangalore*

### *Inside*

- *Estimation of Coda Waves Attenuation For NW Himalayan Region using Local Earthquakes*
- *Receiver Function Analysis of Broadband Seismic Data at Mountabu*
- *Is the Himalayan Arc Really Perfect?*
- *Tectonics of the Himalayan Mountain Front, Darjiling Himalayas, India*
- *Global Positioning System (GPS)-based Crustal Deformation of the Darjiling-Sikkim Himalaya*
- *GPS Measurements in the West Southern Peninsular Shield of India*
- *Estimates of Precipitable Water Vapour from GPS Data over the Indian Subcontinent*
- *Estimates of Plate Velocity and Crustal Deformation in the Indian Sub-continent using GPS Geodesy*
- *GPS Derived Displacements in Andaman Nicobar Islands*
- *Preliminary Estimates of Transient Deformation in Northeast India from GPS Geodesy*

## 2.1 Estimation of Coda Waves Attenuation for NW Himalayan Region using Local Earthquakes

Attenuation of seismic waves in the lithosphere is an important property for the study of regional earth structure. Attenuation of these waves is described by a dimensionless parameter called quality factor Q. This quality factor is inversely proportional to the decay of amplitude (energy) of seismic waves. The inverse of the quality factor is known as attenuation factor ($Q^{-1}$). The quality factor, Q depends upon tectonic and seismic activity of the earth's regional medium. Basically, this parameter is used to estimate the seismo-tectonic activity by utilising the local and regional earthquake data.

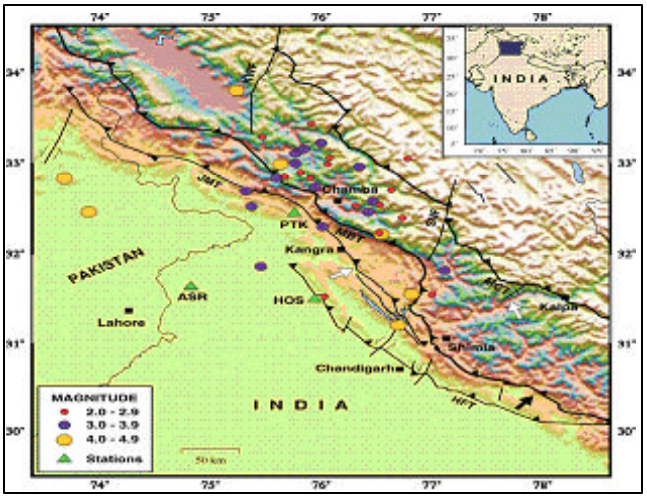


Fig 2.1 General seismotectonic and topographical map of NW Himalayas and adjoining area. MCT: Main Central Thrust; MBT: Main Boundary Thrust; HFT: Himalayan Frontal Thrust; JMT: Jawalamukhi Thrust; KWF: Kisatwar Fault; SNF: Sundarnager Fault; Earthquake epicentres are plotted by circles, triangles represent the recording stations (PTK: Pathankot; HOS: Hoshiarpur; ASR: Amritsar) and cities are shown by squares.

Coda waves are the secondary seismic waves, which are generated by scattering of primary body waves at different hetereogeneities due to refraction, reflection and diffraction. These coda waves have been estimated as backscattered superposition waves from randomly distributed hetereogeneities in homogenous medium. The attenuation of these waves is measured by coda quality factor, Qc. This factor differs locally from one region to another region and in some cases even to azimuths of the station in same region but its variation is not much dependent on the magnitude of small earthquakes. The amplitude of coda waves is effected due to geometrical spreading, earthquake source factor, path propagation and station site effect. After compensating for all these factors the remaining decay of seismic amplitude with lapse time measure the coda wave attenuation. The coda Q is strongly dependent on frequency for heterogeneous medium therefore it is used to assess the discontinuities of the medium. If A(f,t) is the amplitude of wave at central frequency f and lapse time t then its amplitude decay is given by the relation

$$A\{(f,t)*t\} \propto t^{-n} e^{-\frac{pft}{Qc}} \quad \text{or}$$

$$A\{(f,t)*t\} = Kt^{-n} e^{\frac{pft}{Qc}} \quad \text{---------- (1)}$$

where K is a constant, which depends upon earthquake source, path propagation and site effect of the station, n is the geometrical spreading parameter (generally 1.0 for body waves and 0.5 for Surface waves) and Qc is the coda quality factor. By putting n=1 in eq. (1) and taking logarithm of both sides we, get

$$\log(A(f,t)*t) = \log K - \frac{pf}{Qc} t \quad \text{---------- (2)}$$

Therefore by plotting log(A(f,t)*t) values at different lapse times, we can fit a straight line and b (the slope) of the line gives the quality factor Qc by the relation

$$Qc = \frac{pf}{b} \quad \text{---------- (3)}$$

We have calculated the quality factor by using relation (3) for NW Himalayas for 36 local earthquakes of three seismic station data (Fig 2.1). These earthquakes are of magnitude range 2.1 to 4.8 with epicentral distance from 1 to 202 kms. We analysed the data at six central frequencies 1.5,3,6,9,12 and 18 Hz using eight lapse time windows from 25 secs to 60 secs starting from double the S wave time. The estimated average frequency dependence quality factor for NW Himalayan region gives the relation, $Qc=158f^{1.05}$, while this relation varies from $Qc=86f^{1.09}$ at 25 sec

window length to Qc=221f$^{0.91}$ at 60 sec window length for all the stations. The average Qc value with standard deviation at 40 sec window length varies from 133.6±44 at 1 Hz to 3044.0±574 at 18 Hz of central frequencies.

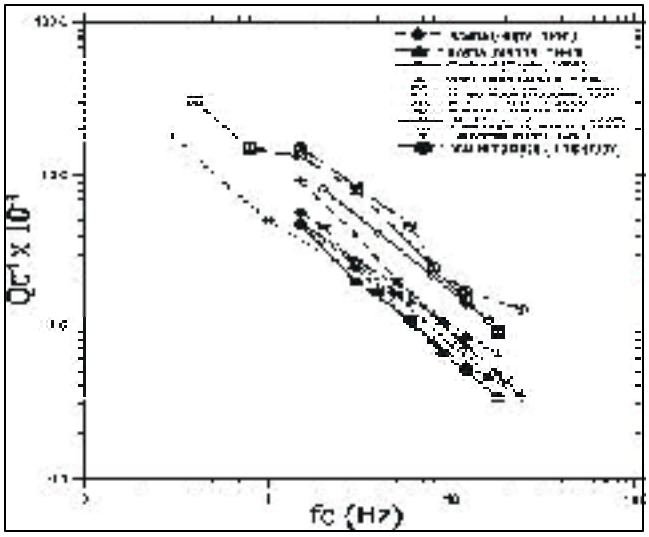


Fig 2.2 Comparison of Coda-Qc of NW Himalayan region with reported coda-Qc of other regions of the world.

The attenuation of coda waves has been observed for different regions of the world by several researchers for tectonic and seismic active regions, high Qc values (e.g. > 600) for seismic inactive stable regions and intermediate values for moderate regions. Our results show that the NW Himalayas is tectonic and seismic active region, while Gangetic plains near NW Himalayas are intermediate active region (Fig 2.2). The attenuation property of Indian lithosphere is also estimated by coda Q method for Garhwal Himalayas, Koyna region and southern Indian region. These observations indicate coda Q values equal to other tectonic and seismic active regions of the world. The coda Q value observed by this study is also comparable to other Indian regions but more sensitive to frequency, which shows that this region is more heterogeneous as compared to other parts of the country.

*Imtiyaz A Parvez and Naresh Kumar*

## 2.2 Receiver Function Analysis of Broadband Seismic Data at Mountabu.

Receiver function analysis is used to image the crustal structures underneath isolated seismic stations. Three component seisograms of teleseismic events with wide bandwidth are used to compute receiver functions by deconvolving the vertical components from the radial and transverse components as the vertical component contains the most of the main P phases while the horizontal components contain the S phase. Firstly, a rotation of the vertical, North-South and East-West components to the propagation direction is carried out in order to get true vertical (Z), Radial (R) and Transverse (T) components. The seismograms recorded are a convolved output of source effect, mantle path effect and near receiver structures. We need to isolate the near receiver structures from the rest and to get this we deconvolve the vertical component from the radial or transverse component. Receiver function is an indirect measure of the depth to the discontinuities.

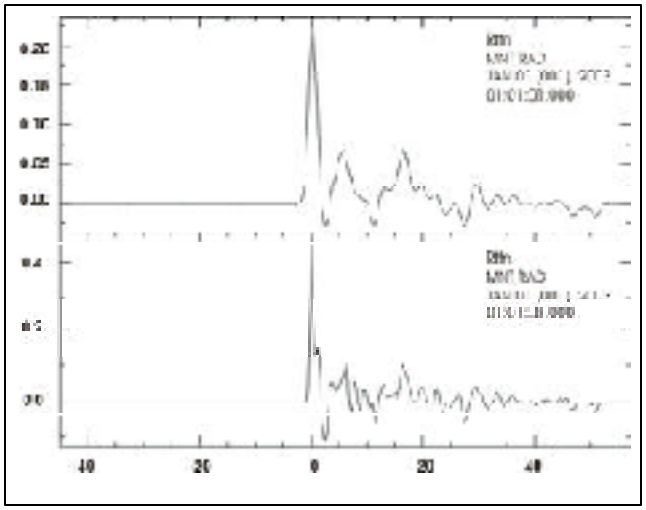


Fig 2.3 Receiver functions obtained at Mountabu. The upper trace is obtained using Gaussian filter 1.0 and lower 2.5.

Two types of deconvolution are commonly used in computational seismology. One in the frequency domain and the other in the time domain. In frequency domain, deconvolution is equivalent to the ratio of the frequency components of the radial R(ω) and vertical components Z(ω) as,

$$E\_R(\omega)=[R(\omega)Z^*(\omega) / Z(\omega) Z^*(\omega)]G(\omega),$$

where G(ω) is the Gaussian filter.

Spiking deconvolution is commonly done in time domain in which the vertical component waveform is compressed to a zero lag spike. The spiking deconvolution operator is strictly the inverse of the initial segment of vertical component that is obtained by minimizing the least square differences

between the observed seismogram and desired delta spike function. Then the acquired inverse filter is convolved with vertical, radial and transverse components to obtain the desired zero lag spike, source equalized radial and transverse receiver function. After deconvolution, we can stack the traces obtained from the same direction to enhance signal to noise ratio. Receiver functions are traditionally inverted to the S wave velocity model that produces an estimation of shear velocity structure under a given seismic station. The inversion requires an initial velocity depth model which then iteratively improves the model by a sequence of relatively thin layers with a gradual increase or decrease of the velocity. The delay time of the direct Ps conversion from the Moho and the crustal multiples can be used to estimate the crustal thickness by a given average crustal P velocity.

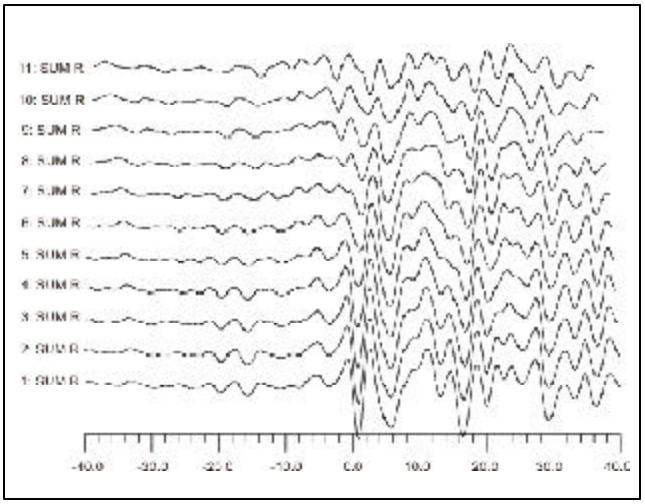

Fig 2.4 Receiver functions obtained using seismic handler at Mountabu. Three clear discontinuities are shown at 5.5, 15 and 30 sec.

We have analysed about 40 teleseismic events occurred in 2002 with magnitude greater than 5 at Mountabu. We used iterative, time-domain deconvolution technique using Seismic Analysis Code (SAC) to produce the P receiver functions. The stack of 17 events with back-azimuth between 100 and 125 is shown in the Fig 2.3. Here, the Ps phases come around 6s after the first P arrival. We also used Seismic Handler (SH) to obtain the P receiver function in order to see if there is any variation in the receiver functions. Here we stack only 9 receiver functions with back-azimuth 100 to 125 and the output is shown in Fig 2.4. The Ps converted phases are coming around 5.5 sec from the main P phase. The other discontinuities are also clearly visible around 15 and 30 sec coming from upper mantle. For the events from other back-azimuth, the time difference for P to Ps is around 6 sec and thus need more data to get reliable information.

This is only a preliminary analysis and after processing more data a clear picture of the crustal structure beneath Mountabu can be obtained. The inversion of the P receiver function is being done.

*Imtiyaz A Parvez and A N Sunaina*

## 2.3 Is the Himalayan Arc Really Perfect?

The India-Eurasia collision Himalayan plate boundary is one of the most active orogens on the earth and is considered to form a near perfect circular arc between longitudes 77.2ºE and 92.1ºE with a radius of 1696±55 km and centre at 42.4±2.1ºN; 91.6 ±1.6ºE. The continuity of this arc has been used to laterally project and extrapolate geological cross-sections and geophysical data along the length of the Himalayan belt. For example, the INDEPTH Himalayan hinterland geometry has been used as the representative Himalayan hinterland geometry in many parts of the Himalayan belt. Continuity of the arc has also been used to compute representative convergence rate of ~ 20 mm/yr along the arc from Global Positioning System (GPS) based geodetic measurements and used to compute Himalayan seismic hazard estimates. Is this realistic over different space and time scales? The Himalayan Mountain front exhibits sinuosity with amplitudes of the order of 10s of kilometers resulting in well-defined salients and recesses pointing to lateral variations in the deformation kinematics of the Himalayan wedge over geological time. The sinuosity of the front causes a variation in the number of thrusts south of the Main Boundary Thrust, making the definition of the Siwalik on Quaternary, Main Frontal Thrust non-unique along the length of the Himalayan front. The presence of transverse zones in the Himalayas also supports variation in deformation kinematics along its length.

Variations in the earthquake epicenter and hypocentre distribution patterns in the Himalayan belt point to lateral variation in deformation kinematics over more recent timescales. GPS based convergence rates also exhibit significant variability along the length of the Himalayan arc ranging from about ~10 mm/yr to ~20 mm/yr. Given this, continuity of the Himalayan arc through different space and time scales may not be a realistic assumption. Averaged over geological time the Himalayan plate boundary is segmented like the fingers of the hand instead and each finger is mechanically distinct from its neighbour and separated from them by transverse zones, lateral or oblique ramps. Consequently, the Himalayan convergence, when averaged over geological time, is likely to be discontinuous with abrupt changes across transverse zones. A non-continuous Himalayan plate boundary over geological time and lateral variation in the deformation kinematics evident from the available geologic, geophysical and seismological data implies that it may be meaningless to project data and geometry of structures laterally from one part of the Himalayas to another, especially across known transverse zones. Complete transects across the Himalayan mountain belt must be made to understand the deformation kinematics in the Himalayas better.

*Malay Mukul*

## 2.4 Tectonics of the Himalayan Mountain Front, Darjiling Himalayas, India

The Himalayan Mountain front in the Darjiling Himalayas exhibits a pronounced frontal recess near Gorubathan. The Gorubathan recess exhibits an amplitude of ~ 15 km and the Siwalik section is not exposed within the recess. Investigations into the cause of the recess has led to the discovery of a new transverse structure at high angles to the trend of the Himalayan belt that continues into the Yadong-Gulu cross structure on the Tibetan Plateau. The Gish river flows along this transverse zone near the mountain front; the Gish transverse zone is expressed as an abrupt discontinuity between low Siwalik hills to the west and plain land to the east. The mountain front to the west of the Gish zone is defined by a thrust that puts Siwalik rocks on Quaternary deposits whereas the mountain front to the east of it is defined by a thrust that puts Proterozoic Daling Formation rocks on Gondwanas. There is evidence of blind imbrication continuing farther south of the mountain front both east and west of the Gish zone; these blind imbricates form E-W trending fault scarps. The Siwalik section is repeated and exposed by several imbricate thrusts west of the Gish zone. These faults are missing east of the Gish fault or blind leading to the absence of Siwalik rocks east of the Gish zone. The mountain front east of the Gish zone is characterized by asymmetric river terraces that have been raised by ~ 400 m relative to the present level of the Chel river. Such terraces are missing west of the Gish zone. The contrasting styles of geological and neotectonic deformation kinematics, reflected also in the topography along the Darjiling Himalayan mountain front, on either side of the Gish zone points to segmentation of the Himalayan deformation along its length. Also, there is no Siwalik-on-Quaternary thrust exposed east of the Gish zone. Therefore, the Main Frontal Thrust cannot be traced unambiguously across the Gish zone; this makes the definition of the Main Frontal Thrust in the Darjiling Himalayas non-unique. The Gish transverse zone exhibits an early quasi-plastic deformation phase characterized by steep, east-dipping discrete cleavage. This is overprinted by elastico-frictional, left-lateral, strike-slip deformation in the Gish zone characterized by widespread cataclasis.

*Malay Mukul and Abdul Matin*

## 2.5 Global Positioning System (GPS)-based Crustal Deformation of the Darjiling-Sikkim Himalaya

Global Positioning System (GPS) based crustal deformation measurements allow the estimation of very short-term deformation from the day measurements are started. The three-dimensional Bangalore (IISc: 13.02 N; 77.57 E) – Lhasa (LHAS: 29.66 N; 91.10 E) baseline is a good proxy for the very-short term active tectonics in the Darjiling-Sikkim and Western Bhutan Himalayas. The ITRF 2000 model for IISc and Lhasa IGS stations for the period 1997-2004 predicts a convergence of ~ 10 mm/year in contrast with the ~ 20mm/year convergence measured from central Nepal and postulated for the entire Himalayas. Campaign-mode GPS studies

carried out in the Darjiling-Sikkim Himalayas between 2000 and 2003 were aimed at resolving the ~10mm/year convergence observed along the IISc-LHAS baseline. The IISc-KYON baseline is a good proxy for convergence accommodation in the Darjiling-Sikkim Himalayas because Kyongnosla (KYON: 27.36 N; 88.714 E) is located along the IISc-LHAS line near the Indo-Tibet-Bhutan border. This line shortened by 5.33 ± 2.9 mm/yr during 2000-2003 indicating that only half of the ~10mm/yr convergence is taken up in the Darjiling-Sikkim Himalayas; this is corroborated by the 6.59 ± 2.85 mm/yr convergence observed along the KYON-LHAS line. The station at Delo Hill (DELO: 27.09 N; 88.50 E) has been monitored in campaign mode since 1997 and a statistically insignificant convergence of 3.07 ± 5.4 mm/yr was measured between 1997 and 1999 between IISc & DELO. 2000-2003 measurements on DELO also revealed a statistically insignificant convergence of 1.29 ± 1.76 mm/yr between IISc & DELO during 2000-2003. The convergence between LHAS and DELO during the same period was 5.67 ± 1.68 mm/yr. This low convergence suggests that although most of the convergence is being taken up north of Delo in the Higher Himalayas, there is probably some convergence being taken up south of Delo that could be resolved through a baseline shorter than the IISc-DELO line. The Mungpu (MUNG: 26. 98 N; 88. 40 E) station was, therefore, set up south of Delo. IISc-MUNG convergence over 2000-2003 was statistically insignificant 1.66 ± 1.94 mm/yr whereas LHAS-MUNG convergence over the same period was 10.1 ± 1.87 mm/yr. The 2000-2003 DELO-MUNG convergence was measured to be 3.83 ± 2.07 mm/yr and, therefore, some convergence is being accommodated between the MUNG and DELO stations. The above results indicate that the frontal part of the Darjiling-Sikkim Himalayas is not accommodating much convergence and most of the 4-5 mm/year convergence is being taken up between 27°N and 27.5°N latitudes. Also, the observed convergence in the Darjiling-Sikkim is significantly lower than that observed in Nepal and western Himalayas.

*Malay Mukul, Sridevi Jade, Abdul Matin and M S M Vijayan*

## 2.6 GPS Measurements in the West Southern Peninsular Shield of India

GPS measurements were carried out (Fig 2.5) to quantify the time evolving deformation field in the southwestern peninsular India towards modelling the ongoing tectonic and seismogenic processes. More than 30 sites lying on either side of the suspected active faults/shear zones such as Mayar-Bhavani, Bavali and Palghat-Cauvery faults/shears were identified for monitoring. In addition, 6 sites earlier established by C-MMACS during 1995 were also measured. These measurements were expected to give long term deformation field (1995-2005) in southern India peninsula in general

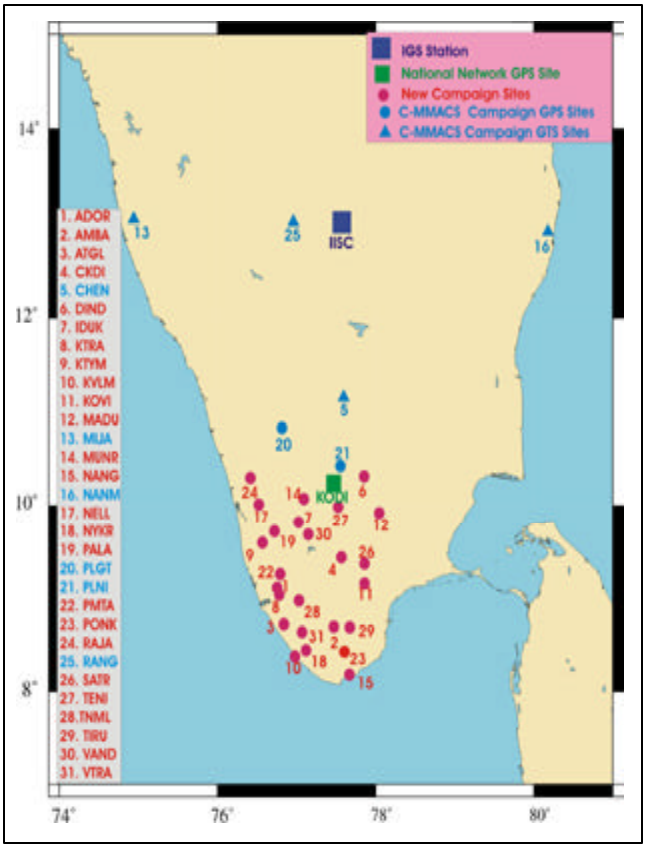


Fig 2.5 GPS Campaign and Permanent sites in South India

and also help identify the suspected major active shear/fault zones in the west southern penisular shield.

*Sridevi Jade, M S M Vijayan, P Dileep Kumar, M Radhakrishna, Nilof S Pasha and Venkateswaran*

## 2.7 Estimates of Precipitable Water Vapour from GPS Data over the Indian Subcontinent

Water vapour distribution is difficult to resolve by conventional means, since water vapour exhibits very high spatial and temporal variability. The growing networks of continuously operating GPS systems, however, offer the possibility of estimating the Integrated Water Vapour (IWV) or, equivalently Precipitable Water vapour (PW). These estimates constitute critical inputs in operational weather forecasting and in fundamental research to model atmospheric storm systems, atmospheric chemistry, and the hydrological cycle. Integrated water vapour has been estimated from GPS data of continuously operating GPS stations established by C-MMACS at Bangalore, Kodaikanal, Hanle and Shillong over the 3-year period (2001-2003).

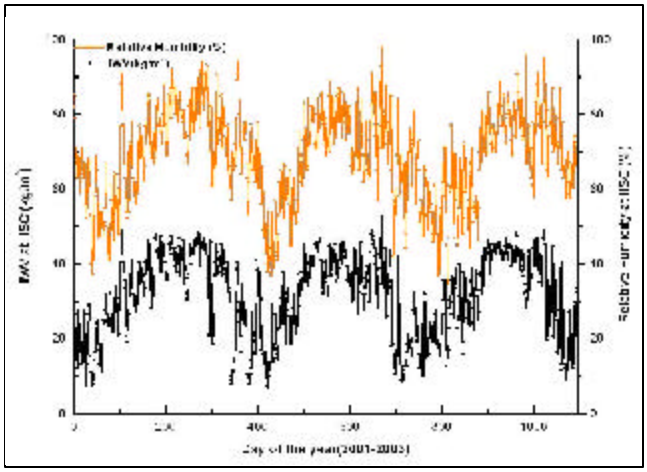

Fig 2.6 Time series of GPS derived IWV estimates and ground humidity for Bangalore (2001-2003)

GPS derived Integrated water vapour estimation at four GPS sites geographically spread across the Indian subcontinent (Fig 2.6 to 2.8) show the variability of water vapour across the sites with Bangalore having the highest value, Hanle the lowest and Shillong and Kodaikanal having intermediate values, each corresponding well with its geographical location. Water vapour variations over the year for all the 3 years (Fig 2.6) roughly correspond to the Indian monsoon period with December to March being the dry season and June to October the peak monsoon period, and the intervening months marking a transitional period. The Interannual variability of IWV (Fig 2.8) over the

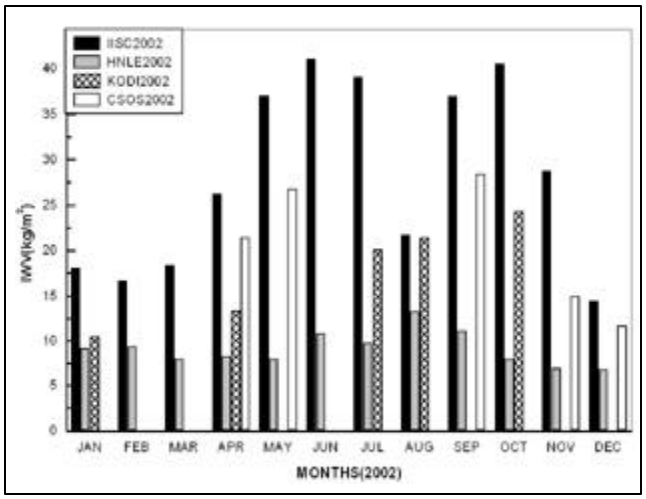


Fig 2.7 Monthly average of IWV values for the four GPS sites

3 years roughly corresponds to the Indian monsoon intensity with 2002 being the lean one. GPS derived IWV values presented here, are the first such determination over the Indian subcontinent.

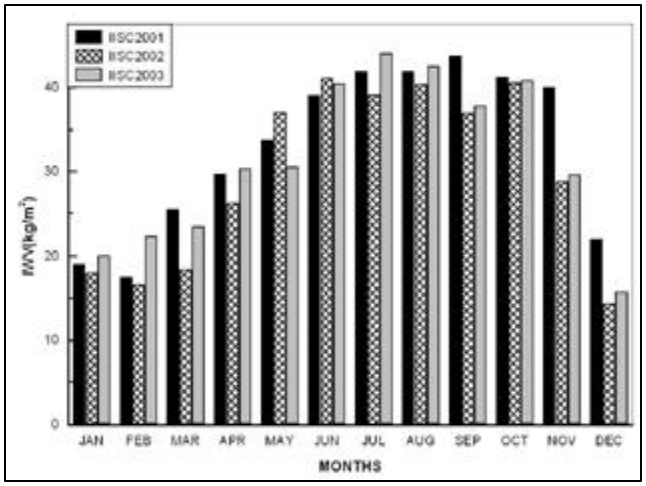


Fig 2.8 Inter annual variability of GPS derived IWV estimates for Bangalore

With consistent data analysis in terms of methods and models, ground-based GPS will, as the length of the time series grows, become an independent data source in climate monitoring. Meanwhile, simulation experiments designed to assess the quality improvement of forecasts when GPS derived IWV data are incorporated, may generate insightful ideas as to how best may one fruitfully exploit the potential possibilities.

*Sridevi Jade and M S M Vijayan*

## 2.8 Estimates of Plate Velocity and Crustal Deformation in the Indian Sub-continent using GPS Geodesy

GPS data collected at C-MMACS from 1994 to 2002 has been analysed and the results obtained have been integrated to give an overall picture of crustal deformation and plate velocity in the Indian Sub-continent. Notable conclusions that arise from the analaysis are as follows. Southern peninsular India moves as a rigid plate with the velocity approximately equal to Indian plate velocity and regional deformation in southern peninsula is negligible. Convergence rates in Himalaya indicate that significant amount of India and Eurasia convergence is accommodated here. GPS derived velocity and deformation rates in the Himalayan arc vary from west to east suggesting the deformation mechanisms in Ladakh, Garhwal, Kumaun and Sikkim Himalayas are different and are to be treated differently. GPS derived extension vector between the Himalayan sites and Lhasa is consistent with the east west extension of southern Tibet. Kachchh GPS results give post seismic deformation consistent with Bhuj rupture zone as GPS measurements were made after the 2001 earthquake and one more epoch of GPS measurements are needed to determine long term plate deformation. GPS measurements in the north -west and north-east India are insufficient, nevertheless velocities of Jamnagar and Shillong indicate significant deformation in these regions.

*Sridevi Jade*

## 2.9 GPS Derived Displacements in Andaman Nicobar Islands

The devastating $M_w$ 9.0 Sumatra earthquake of 26th December 2004 which occurred as thrust faulting on the interface of Indian plate and Burma microplate and the tsumani has claimed many lives. GPS field measurements were made in Andamans at Port Blair campaign site by C-MMACS since 1996. In September 2003 Andaman GPS measurements were extended to five Campaign sites. These campaign sites were remeasured in February 2005 after the earthquake to determine the displacement due to the earthquake and the after shocks which occurred over a zone of 1300KM. During the 2005 campaign, four sites (Diglipur, Chatham Island, Havelock Island and Car Nicobar) were remeasured

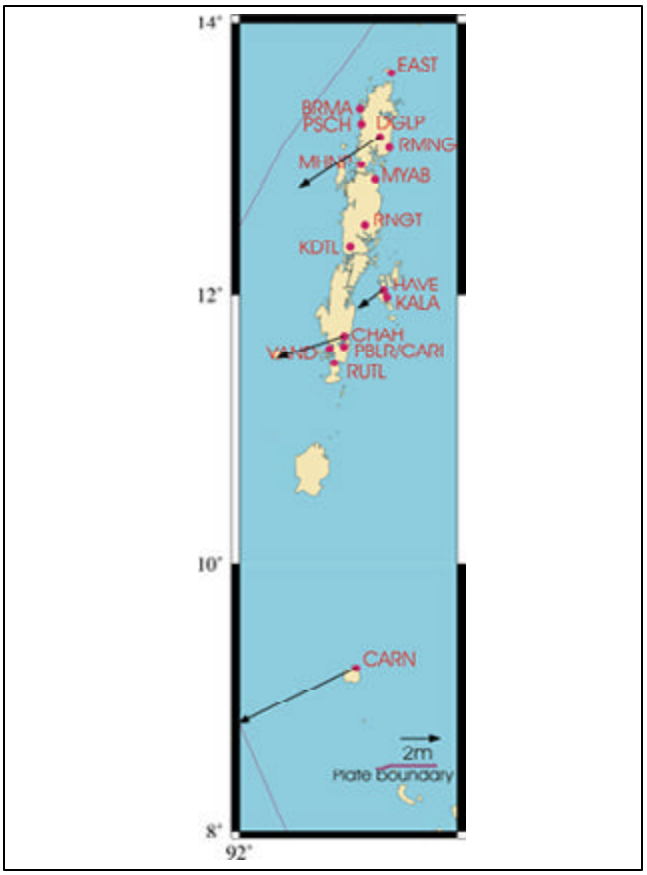


Fig 2.9 GPS derived horizontal displacement vectors in Andaman/Nicobar Islands with Campaign sites

and eleven new sites were established in Andamans (Fig 2.9) to monitor the post seismic deformation. The results from the rigorous data processing and analysis of the GPS data indicates that the coseismic displacement (Fig 2.9) of all the four stations are in south west direction and magnitude is in the order of 1.6m ± 10mm to 6.5m ± 5mm. The height component indicates uplift for the Diglipur station in north Andamans and subsidence at Chatham Island and Car Nicobar. These GPS derived cosiesmic displacements precisely quantify the slip, uplift and subsidence of the 2004 rupture which from preliminary news paper reports is estimated to be 7 to 23 m slip , 1 to 4m subsidence in Nicobar Islands and 1 to 2 m uplift in Andamans Islands.

*Sridevi Jade, M B Ananda, P Dileep Kumar, Souvik Banerjee and V K Gaur*

## 2.10 Preliminary Estimates of Transient Deformation in Northeast India from GPS Geodesy.

The Northeastern part of Indian subcontinent is one of the most seismically active regions of the world with occurrence of several earthquakes. It lies at the junction of Himalayan Arc to the north and Burmese Arc to the east. This region has experienced 18 large earthquakes (M =7) during the last 110 years, which includes the 1897 Shillong earthquake, and 1950 Assam-Tibet border earthquake . High Seismicity in northeast India is attributed to collision between Indo-Eurasian plates and subduction tectonics along the Indo-Burmese Arc. In light of the above, it is important to study the present day deformation in northeast India to answer the questions related to the potential seismic hazard. With this in mind, GPS measurements were made at eight permanent stations and six campaign sites in Northeast India from 2002-2004 to quantify the deformation in Shillong Plateau, Arunachal Pradesh and Indo-Burmese Arc. Preliminary estimates of transient deformation show no active deformation in Shillong Plateau, statistically insignificant deformation between the northeast permanent network sites in and around Shillong Plateau, 5 ± 1mm/yr convergence between Shillong plateau and Sikkim, Baselines between Indo-Burmese Arc and Shillong indicate a variation in shortening rate (1 to 11mm/yr) as we move from Tripura salient to Naga Schuppen belt. Baselines with IGS site Lhasa indicate a lateral variation in the shortening rate as we move from west to east. These results give for the first time GPS derived deformation and motion rates in northeast India.

*Sridevi Jade, Malay Mukul, Saigeetha Jaganathan, Anjan Kumar Bhattacharya, M S M Vijayan and V K Gaur*